

RESEARCH ARTICLE

The Role of *HOXB9* and *miR-196a* in Head and Neck Squamous Cell Carcinoma

Lav Darda¹, Fahad Hakami¹, Richard Morgan², Craig Murdoch³, Daniel W. Lambert¹, Keith D. Hunter^{1,4*}

1 Unit of Oral and Maxillofacial Pathology, School of Clinical Dentistry, University of Sheffield, Sheffield, United Kingdom, **2** Institute of Cancer Therapeutics, University of Bradford, Bradford, United Kingdom, **3** Unit of Oral and Maxillofacial Medicine & Surgery, School of Clinical Dentistry, University of Sheffield, Sheffield, United Kingdom, **4** Department of Oral Pathology and Biology, University of Pretoria, Pretoria, South Africa

* k.hunter@sheffield.ac.uk



Abstract

Background

Previous studies have demonstrated that a number of *HOX* genes, a family of transcription factors with key roles in early development, are up-regulated in head and neck squamous cell carcinoma (HNSCC) and other cancers. The loci of several Homeobox (*HOX*) genes also contain microRNAs (miRs), including miR-196a.

Methods

Global miR expression and expression of all 39 *HOX* genes in normal oral keratinocytes (NOKs), oral pre-malignant (OPM) and HNSCC cells was assessed by expression microarray and qPCR and in tissues by immunohistochemistry (IHC) and qPCR of laser microdissected (LCM) tissues. Expression of miR196a and *HOXB9* was reduced using anti-miR-196a and siRNA, respectively. Expression microarray profiles of anti-miR196a and pre-miR196a transfected cells were compared to parental cells in order to identify novel targets of miR-196a. Putative miR196a targets were validated by qPCR and were confirmed as binding to the 3'UTR of miR196a by a dual luciferase reporter assay combined with mutational analysis of the miR-196a binding site.

Results

miR-196a and *HOXB9* are highly expressed in HNSCC compared to NOKs, a pattern also seen in HNSCC tissues by *HOXB9* IHC and qPCR of miR-196a in LCM tissue. Knock-down of miR-196a expression decreased HNSCC cell migration, invasion and adhesion to fibronectin, but had no effect on proliferation. Furthermore, knock-down of *HOXB9* expression decreased migration, invasion and proliferation but did not alter adhesion. We identified a novel primary mRNA transcript containing *HOXB9* and *miR196a-1* as predicted from *in-silico* analysis. Expression array analysis identified a number of miR196a targets, including

OPEN ACCESS

Citation: Darda L, Hakami F, Morgan R, Murdoch C, Lambert DW, Hunter KD (2015) The Role of *HOXB9* and *miR-196a* in Head and Neck Squamous Cell Carcinoma. PLoS ONE 10(4): e0122285. doi:10.1371/journal.pone.0122285

Academic Editor: Andrew Yeudall, Virginia Commonwealth University, UNITED STATES

Received: November 6, 2014

Accepted: February 10, 2015

Published: April 10, 2015

Copyright: © 2015 Darda et al. This is an open access article distributed under the terms of the [Creative Commons Attribution License](https://creativecommons.org/licenses/by/4.0/), which permits unrestricted use, distribution, and reproduction in any medium, provided the original author and source are credited.

Data Availability Statement: The microarray data described in this paper is held in public repositories: NCBI GEO database (accession numbers GSE52811 and GSE52810).

Funding: The authors received no specific funding for this work.

Competing Interests: The authors have declared that no competing interests exist.

MAMDC2 and *HOXC8*. We confirmed that *MAMDC2* is a novel miR-196a target using a dual luciferase reporter assay with the effect abolished on mutation of the binding site.

Conclusions

These results show that *miR-196a* and *HOXB9* are overexpressed, perhaps co-ordinately, as HNSCC develops and exert a pro-tumourigenic phenotype in HNSCC and OPM cells.

Introduction

The identification of a number of key molecular alterations in cancer has resulted in major advances in diagnosis and targeted therapy with validated biomarkers, heralding the advent of personalised medicine. However, head and neck squamous cell carcinoma (HNSCC) lags behind, with no consistent oncogenic drivers identified and cetuximab being the only approved targeted therapeutic. This reflects both the molecular heterogeneity of this cancer and the paucity of understanding of its molecular landscape [1]. Worldwide, HNSCC presents a significant public health problem, being the 6th most common cancer with survival rates which have not improved significantly for several decades [2]. Hence, there is a pressing need to find both novel targets for therapeutic intervention and new biomarkers in HNSCC.

Data mining of our published gene expression profile of normal, premalignant and HNSCC cells (<http://bioinformatics.picr.man.ac.uk/vice/PublicProjects.vice?pager.offset=15>) to identify deregulated pathways [3] has identified a number of consistently up-regulated transcription factors in HNSCC, including several Homeobox (*HOX*) genes (see Hunter et al, Supplementary data S3 and S4). *HOX* genes code for transcription factors with important roles in embryogenesis and organogenesis [4,5]. There are 39 *HOX* genes present on chromosomes 2, 7, 12 and 17, split into four clusters (A-D), and further sub-divided into 13 paralogous groups [4,6]. *HOX* proteins contain a 60 amino acid homeodomain that facilitates their binding to DNA [7]. *HOX* gene products interact with co-factors such as *PBX*, a member of the *TALE* family of homeodomain proteins, which alters their binding with DNA, regulates transcription and is needed for specific *HOX* functions [8].

HOX gene expression is dysregulated in many cancers, most significantly in leukaemia. In acute myeloid leukaemia (*AML*), fusion proteins of *NUP98:HOXC11* and *NUP98:HOXD13* have been identified which result in aberrant *HOX* trans-regulatory activity [9,10]. In breast cancer, *HOXA5* and *HOXB13* expression is down-regulated [11,12] whereas *HOXB9* is highly up-regulated [13] and changes in *HOX* gene expression have been reported in lung [14,15] and gastric cancer [16]. In HNSCC, several *HOX* genes show higher levels of expression in pre-malignant and cancer tissues compared to normal tissues [17]. Overall, 18 *HOX* genes were more highly expressed in HNSCC cells than in normal cells, among them *HOXB9*. However there is a lack of clarity in the literature as to the extent and relative importance of *HOX* genes in HNSCC carcinogenesis.

HOX clusters also contain microRNAs; non-coding RNA transcripts which bind predominantly to the 3'UTR of target transcripts [18–21], resulting in translational repression or degradation of the mRNA transcript [19]. MicroRNA (miR)-196 is present in three *HOX* clusters: miR-196b on 7p15 (*HOXA*), miR-196a-1 on 17q21 (*HOXB*) and miR-196a-2 on 12q13 (*HOXC*). miR-196a-1 and miR-196a-2 have an identical mature sequence, whereas miR-196b differs by a single nucleotide [22]. These miRNAs target *HOX* genes located 5' of their locus, supporting the theory of posterior prevalence [21,23]. miR-196a targets several *HOX* genes,

including *HOXA5*, *HOXB7*, *HOXB8* and *HOXC8* [18,19,24,25] and has also been shown to directly target several other genes such as *ANXA1*, *p27*, *KRT5*, *S100A9* and *SPRR2C* [20,26,27]. Expression of miR-196a is up-regulated in breast, gastric, lung and oesophageal cancers [16,20,25,28], whereas it is down-regulated in melanoma [29]. miR-196a has been shown to be up-regulated in HNSCC and may also be detected in the serum of these patients pre-operatively [22,30]. In a recent meta-analysis of miR profiling in HNSCC tissues, miR196a was identified, but only in a minority of the studies assessed. Severino *et al* have shown that transfection of miR196a into normal oral keratinocytes decreases proliferation, but with no effect on the expression of previously described miR196a targets [30]. Thus, the functional consequences of miR-196a alteration in HNSCC and the protein-coding targets mediating any phenotypic changes remain to be fully determined.

In this study, we show that miR-196a and *HOXB9* are the most markedly differentially expressed miR and *HOX* gene respectively when comparing HNSCC and NOKs. This up-regulation was also seen in head and neck cancer tissue compared to normal tissue and bioinformatics analysis suggests that these may be co-expressed (Ensembl Transcript: RP11-357H14.19-001). Thus, we aimed to evaluate the functional effects of high miR196a and *HOXB9* expression in HNSCC and to identify novel and direct targets of miR-196a in this malignancy.

Materials and Methods

Cell culture and tissue samples

B16, B22, B56 (BICR56), T4 (HNSCC cell lines, Beatson Institute for Cancer Research [31,32]), H357 (HNSCC cell line from Prof S Prime [33]), D19, D20, D4, D35 (oral pre-malignant (OPM) cell lines, Beatson Institute for Cancer Research [34,35]), primary normal oral keratinocytes (NOKs; isolated as previously described [36], grown with irradiated 3T3 cells), and OKF4 (immortalized normal oral keratinocytes; iNOK; from J Rheinwald, Boston, USA [37]) were maintained in keratinocyte growth medium (KGM) consisting of DMEM supplemented with 23% Ham's F-12, 10% FCS, L-glutamine (2mM), adenine (0.18mM), hydrocortisone (0.5µg/ml) and insulin (5µg/ml) (all Sigma Aldrich, Poole, UK). CAL27 (HNSCC cell line, ATCC) was maintained in High glucose containing DMEM supplemented with 10% FCS and L-glutamine (2mM). All cell lines were incubated at 37°C and 5% CO₂. None of the cell lines used had a published STR profile, thus we conducted baseline STR profiling to assure no similarity with any other cell line with a known profile. This was conducted immediately prior to the experiments described below. Further information of the cells lines used in this study can be found in [S1 Table](#).

A tissue microarray consisting of 25 oral cavity HNSCCs was available for *HOXB9* immunohistochemistry. The clinicopathological details of this cohort are presented in [S2 Table](#). Three cores from the body of the tumour and 3 cores from the advancing edge were available for each sample. A cohort of normal oral mucosal biopsies was used for comparison, with a site distribution matching the HNSCC cohort. A further cohort of 16 HNSCC ([S3 Table](#)) with site matched normal oral mucosa (from different patients) was used for the assessment of miR196a expression in tissues.

RNA isolation and quantitative RT-PCR

Total RNA was extracted using the RNeasy mini kit (Qiagen, Manchester, UK) and quantified using a NanoDrop Spectrophotometer (Thermo Scientific, Hemel Hempstead, UK). High capacity RNA-to-cDNA kit (Life Technologies, Paisley, UK) was used for cDNA synthesis from total RNA. For miRNA cDNA synthesis, 10ng RNA was reverse transcribed using miRNA-

specific primers. For total cDNA synthesis, 200ng RNA was reverse transcribed using random primers. Quantitative gene expression analysis was performed using SYBR[®] green or Taqman with appropriate controls (U6 for SYBR and RNU48 (Taqman ID: 001006) for Taqman analysis; hsa-miR-196a (Taqman ID: 241070)). Initial screening for all HOX genes was by SYBR green qPCR on a Stratagene platform MX3005p (primers sequences in [S4 Table](#) [14]). Additional qPCR was performed using an ABI 7900HT (Life Technologies, Paisley, UK) and the relative expression of genes, normalised to the abundance of the relevant control transcript, was calculated using RQ Manager 1.2.1 (Life Technologies, Paisley, UK).

Affymetrix miRNA array

RNA from duplicate cultures of NOK (normal OKs), Cal27 and BICR56 (both HNSCC) extracted using the mirVana miRNA isolation kit (Life Technologies, Paisley, UK) and was then prepared as per the manufacturer's protocols (http://media.affymetrix.com/support/downloads/manuals/flashtag_user_guide.pdf) prior to hybridisation onto the Affymetrix GeneChip miRNA 1.0 Array. The array data was normalised using RMA (RMAExpress) and then loaded into tMeV (Craig Venter Institute, Rockville, CA) and analysed using the statistical analysis of microarray tool (SAM) with a false discovery rate <1% and fold change of >5, comparing NOK with HNSCC. The primary data is available in the NCBI GEO database (accession number GSE52811).

HOXB9-miR-196a-1 primary transcript

To investigate the presence of a common *HOXB9*-miR-196a-1 primary transcript (PT), primers were designed that spanned the 6.3Kb between *HOXB9* exon1 and miR-196a-1 precursor transcript (forward: 5' AATTAGGTAGTTTCATGTTGTTGGGCC 3'; reverse: 5' ATAA TAGCTGCTAAGCGTCCC AGAAAT 3'). For the reverse transcription step, primary transcript primers were used with M-MLV reverse transcriptase (Promega, Southampton, UK), followed by PCR using the same primers (product 6.3kb). Nested primers were designed to give a 295bp product within this transcript (forward: 5' AAAGTCAGGGCAGGAGAGGGAAGGG GAA 3', reverse: 5' CAATTTGCCAGCCCTATGAAGTCTGCT 3'), with RNaseA treated (RNA was incubated for 1 hour at 37°C with 100µg/ml RNaseA (Promega, Southampton, UK) and no-reverse transcriptase (RT) controls. The PCR products were separated on a 2% (w/v) agarose gel, visualised under UV transillumination and purified using gel extraction kit (Bioline, London, UK). This product was then cloned into TOPO TA Cloning vector (Life Technologies, Paisley, UK) and positive colonies were selected using blue/white screening, purified using Isolate plasmid mini kit (Bioline, London, UK) and sequenced.

Laser Capture Microdissection (LCM)

Fresh 4µM sections of formalin-fixed, paraffin-embedded (FFPE) tumour and normal tissue (as described above) were de-waxed, stained with haematoxylin and dehydrated by xylene. LCM was carried out using a Pixcell II LCM system (Arcturus, Life Technologies, Paisley, UK). RNAqueous[®] Micro kit (Life Technologies, Paisley, UK) was used to extract RNA from the cells, according to the manufacturer's instructions.

Protein extraction and western blotting

RIPA buffer (Sigma Aldrich, Poole, UK) containing protease and phosphatase inhibitors (Roche, West Sussex, UK) was added to the cell pellet on ice and then centrifuged at 13,000rpm for 5 min at 4°C. The protein was quantified using BCA method [38] as per

manufacturer's protocol (Thermo Scientific, Hemel Hempstead, UK). 40 µg of total protein was loaded onto a 12% (v/v) SDS-PAGE gel. Wet transfer for 1h at 30V transferred protein to a nitrocellulose membrane, before incubation for 1h in blocking buffer (5% (w/v) dried milk with 3% (w/v) BSA in tris buffered saline containing 0.05% (v/v) tween-20) and incubation overnight at 4°C with the primary monoclonal antibody anti-HOXB9 (1:500 in blocking buffer, Abcam, Cambridge, UK) or anti-β-actin (1:3,000 in blocking buffer, Sigma Aldrich, Poole, UK). The membrane was then incubated in horseradish peroxidase-conjugated anti-rabbit IgG (1:3000 in blocking buffer) for 1h and developed with SuperSignal West Pico chemiluminescent substrate (Thermo Scientific, Hemel Hempstead, UK).

Immunohistochemistry (IHC)

Antigen retrieval was performed using a pressure cooker [39] on sections followed by incubation with anti-*HOXB9* (1: 400, Sigma Aldrich, Poole, UK) overnight at 4°C. Vectastain Elite ABC rabbit IgG kit (Vector Laboratories Inc. Burlingame, CA, USA) was used for secondary antibody (30min at room temperature), followed by colour development by DAB reagent (Vector Laboratories Inc. Burlingame, CA, USA). Submandibular salivary gland and sections with no primary antibody were used as positive and negative controls respectively. IHC was analysed by the semi-quantitative modified Quickscore method on 6 cores from each tumour [40].

Anti-miR and siRNA transfection

B16, D19 or OKF4 cells were seeded in a 6-well plate and incubated overnight. Keratinocytes were transfected when 50–70% confluent with anti-miR-196a or pre-miR-196a (50nM, Life Technologies, Paisley, UK) or siRNA targeting human *HOXB9* (50nM, Sigma Aldrich, Poole, UK) using Oligofectamine (Life Technologies, Paisley, UK) according to the manufacturer's protocol. A random, non-targeting negative control sequence (Life Technologies, Paisley, UK) was used in all experiments. Cells were transfected and incubated for 48h in DMEM supplemented with 20% FCS before being used for the functional assays.

Proliferation Assay

Cells were seeded in a 96-well plate (Corning Inc, Corning, NY, USA) in triplicate for each time point (0, 24, 48, 72 and 96h) at a density of 5×10^3 cells in DMEM media supplemented with 10% (v/v) FCS. MTS reagent (Promega, Southampton, UK) was added to the wells, incubated for 1h and then read at 490nm on a Tecan Infinite M200 spectrophotometer (Tecan, Männedorf, Switzerland) using Magellan software.

Adhesion Assay

A 96-well plate was coated with 0.1% (w/v) fibronectin (Sigma Aldrich, Poole, UK) in PBS (1:100) and incubated overnight at 4°C. The following day wells were washed with PBS and incubated with DMEM containing 1% (w/v) BSA for an hour. The transfected cells were plated in triplicate at a density of 3×10^4 cells/well in DMEM and incubated for 1h. Non-adherent cells were removed by washing with PBS. MTS reagent (Promega, Southampton, UK) was added to the wells, incubated for 1h and then read at 490nm on a Tecan Infinite M200 spectrophotometer.

Transwell Migration and Invasion Assay

To assess migration, transfected cells (8×10^4) in DMEM with 0.1% (w/v) BSA were placed, in duplicate, in the top chamber of a 24-well transwell insert (8µM pore size; BD Biosciences,

Oxford, UK). The bottom of the 24-well plate was filled with DMEM supplemented with 2% (v/v) FCS and the cells incubated overnight at 37°C. For invasion assays the top chamber of a transwell insert was covered with 100µL of growth factor reduced matrigel (BD Biosciences, Oxford, UK) and incubated overnight at 37°C. 8×10^4 transfected cells in 0.1% (w/v) BSA in DMEM were placed in the top chamber in duplicate. DMEM containing 2% (v/v) FCS was placed in the bottom of the 24-well plate followed by 48h incubation at 37°C. Mitomycin C (1µg/mL) was added to the medium in both chambers. For both assays the migrating or invading cells present on the underside of the transwell insert were stained with crystal violet and then counted at four random fields by light microscopy.

Agilent Gene expression microarray

The quality of total RNA was assessed using an Agilent Bioanalyzer, (Agilent, Wokingham, UK) with QC thresholds 28s:18s $\geq 2:1$ and RIN = 10. Biological triplicates of B16 and D19 cells were transfected with anti-miR-196a and negative control, whereas OKF4 cells were transfected with pre-miR-196a and negative control in duplicate (total 16 samples). Samples were prepared and hybridised to Agilent oligonucleotide microarray chips (Sureprint G3; Agilent, Wokingham, UK) according to the manufacturer's protocol (http://www.chem.agilent.com/library/usermanuals/public/g4140-90041_one-color_tecan.pdf). Data was loaded into Qlucore Omics Explorer (Qlucore AB, Lund, Sweden) and, following normalisation and principle component analysis, T-test ($p < 0.01$, with multiple test correction) was used to compare the transfected with the parental cells for each cell line. The top 50 up- and down-regulated genes were selected for further validation by qPCR. The primary data is available in the NCBI GEO database (accession number GSE52810).

Luciferase reporter assay and site directed mutagenesis

The *MAMDC2* 3'UTR was amplified using cDNA from B16 cells (primers: wt forward 5' AAA AAAAAA CGCGTAAATGATCTGCATTGGATTTACT 3' and wt reverse 5' AAAAAAAA GTTTAAACAAGATTTT CAAATTATTTTTATTAGGTAATTTTATAATTTTC 3' containing MluI and PmeI restriction sites, respectively). The amplified PCR product was ligated into pMIR-REPORT (Ambion). The miR-196a binding site within the *MAMDC2* 3'UTR was mutated using PCR-based site-directed mutagenesis. pMIR REPORT cloned with wt 3'UTR was used as the template in the PCR. The primers used for mutation of the miR-196a binding site had T_m of $> 78^\circ\text{C}$ (*MAMDC2* mutant forward: 5' CCTTCTTTA TTCCCCCTTTGAGA CGCTTTTGAAGTCACTATAGC 3' and *MAMDC2* mutant reverse: 5' GTCAT AGTGA TTCAAAGCGTCTCAAAGGGGGAATAAAGAAGG 3', mutated bases in bold). The PCR product was incubated for 1h with DpnI (New England Biolabs, Herts, UK) to degrade methylated template plasmid. 500 ng of pMIR vector (wt or mutant) was transfected into B16 HNSCC cells with 50 ng of pRL-TK Renilla luciferase vector (Promega, Southampton, UK) and pre-miR-196a or scrambled negative control (50nM) (Life Technologies, Paisley, UK) using Fugene HD transfection reagent (Promega, Southampton, UK). The cells were incubated for 48h and then the luciferase activity for firefly and renilla was measured using dual luciferase reporter assay (DLRA) (Promega, Southampton, UK) according to the manufacturer's protocol. The assay was repeated thrice in triplicate.

Statistical Analysis

Non-parametric Mann-Whitney U test was performed on the IHC tissue sample scoring for HOXB9 and the absolute value of the qPCR performed on LCM tissue sample for miR-196a.

Parametric student's t-test was used to calculate all other significance values. Results were only considered significant if $p < 0.05$.

Ethics Approval

Ethics approval for the use of biopsy tissues in this study was obtained from The West Glasgow LREC (ref: 08/S0709/70). Ethical approval for the normal oral keratinocyte primary cultures used was obtained from the National Research Ethics Service, UK: 09/H1308/66 and human tissue was used with written, informed consent. The Ethics Approval waived the need for specific consent in both cases as the material to be used was anonymised and surplus to diagnostic requirements.

Results

miRNA microarray analysis reveals high miR-196a expression in HNSCC-derived cell line

MicroRNA profiling using the Affymetrix miRNA array identified a number of significantly differentially expressed miRs between the NOKs and HNSCC cells (Fig 1A). As the number of samples was small the stringency applied in analysis was high (FDR < 1%), in order to robustly identify differentially expressed miRs for further analysis. The number of hits was further limited to those that changed ≥ 5 fold, finally identifying miR-196a, miR-34a and miR-708, as being differentially expressed (Fig 1B). Of these, only miR-196a was highly expressed in HNSCC. Validation of miR-196a expression by qPCR in a full panel of NOK, OPM and HNSCC cells showed high expression in all HNSCC cells tested with variable expression in OPM cells, two

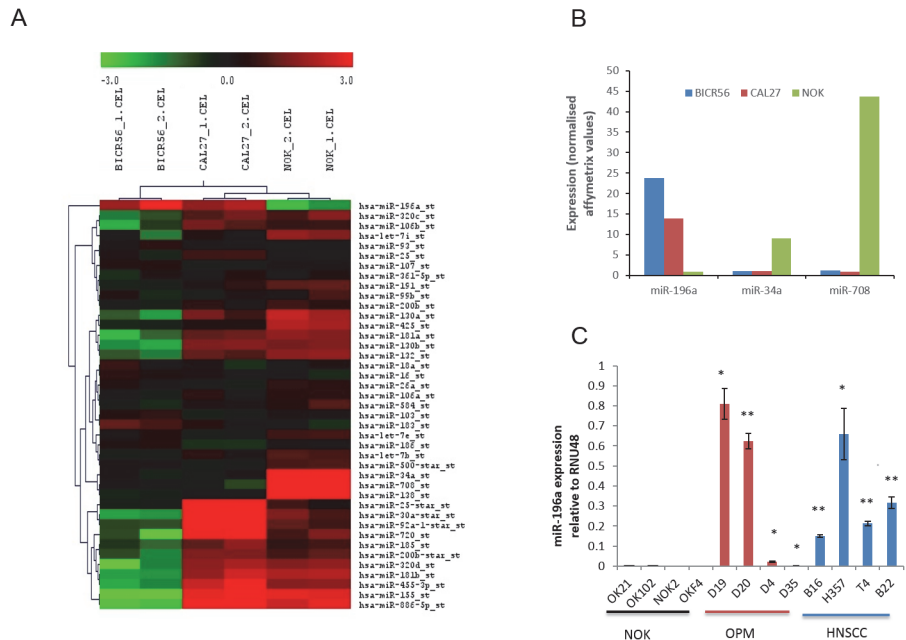


Fig 1. miR-196a is up-regulated in OPM and HNSCC-derived cell lines. **1A:** Heat map showing differentially expressed microRNAs in microarray data from Affymetrix miRNA array on comparison of HNSCC and NOK using SAM with a FDR of 1%. BICR56 and CAL27 are HNSCC cells and NOKs are normal oral keratinocytes. The values presented are the mean of 2 technical replicates. **1B:** Candidate miRNAs were selected as differentially expressed with a FDR of 1% and fold change ≥ 5 . **1C:** Expression of miR-196a in a panel of NOK, OPM and HNSCC cells. * $p < 0.05$, ** $p < 0.01$.

doi:10.1371/journal.pone.0122285.g001

of which had similar expression to that seen in the HNSCCs (Fig 1C). Expression in NOKs was consistently low.

HOXB9 is the most highly expressed of a number of HOX genes elevated in HNSCC-derived cell lines

Expression analysis of all 39 HOX genes revealed that all were more highly expressed in HNSCC compared to NOK (Fig 2A and S2 Fig). The highest differential expression seen was of HOXA4 (291 fold, $p < 0.01$), HOXA5 (105 fold, $p < 0.01$), HOXA9 (155 fold, $p < 0.001$), HOXB9 (1293 fold, $p < 0.001$), HOXC9 (41 fold, $p < 0.01$) and HOXD10 (23 fold, $p < 0.01$), all of which are well recognised in the literature [7,17,41,42], but there was marked variability in the extent of the fold change. HOXB9 was the most markedly differentially expressed, on average > 1000-fold higher than in NOK. This was validated by qPCR, which demonstrated consistently high gene expression of HOXB9 in OPM and HNSCC cells (Fig 2B). Despite a lack of direct correspondence in HOXB9 protein levels (particularly for B16), the difference in expression

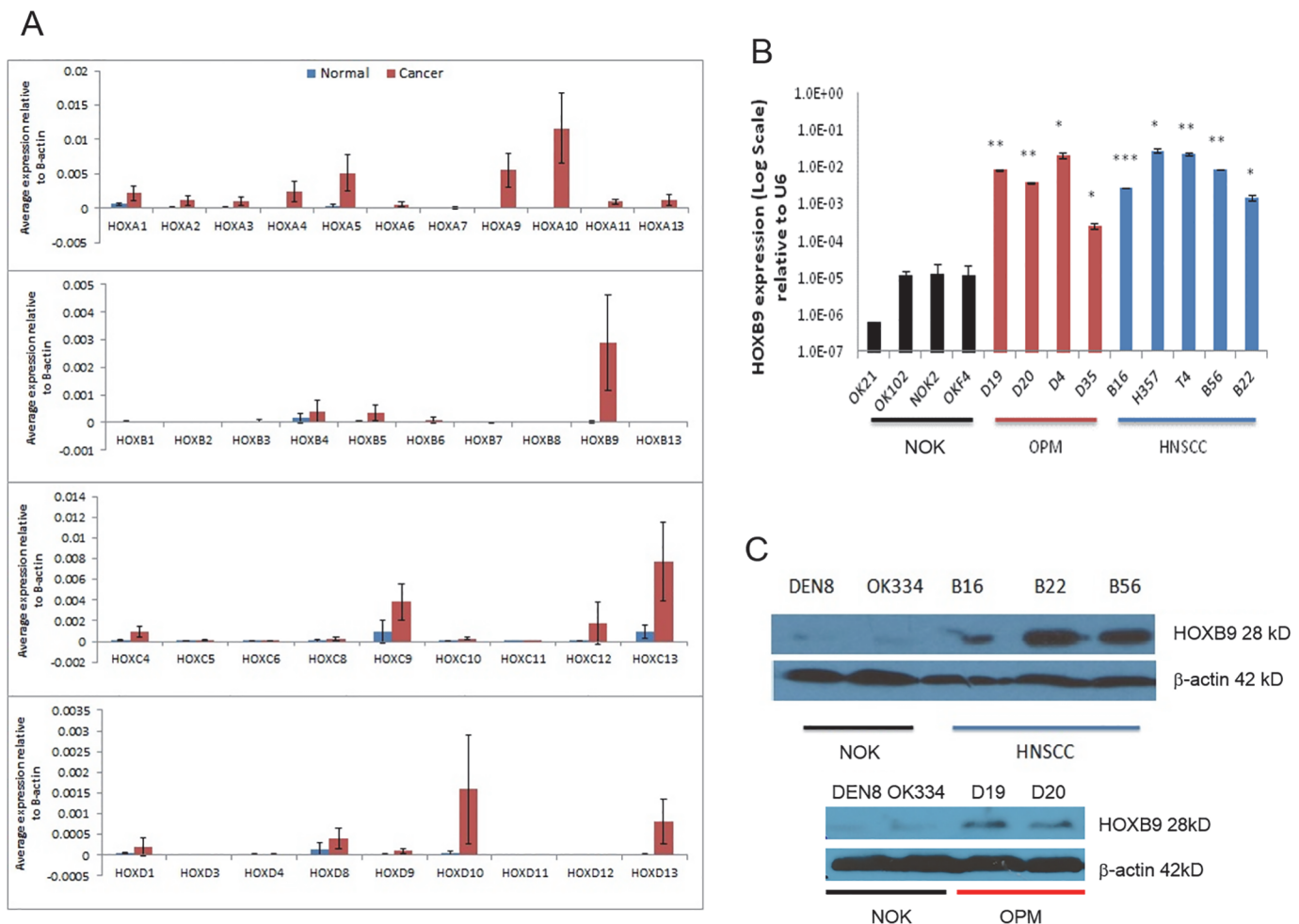


Fig 2. HOXB9 is over-expressed in OPM and HNSCC-derived cell lines. **2A.** Overall mean expression of all 39 HOX genes as measured by qPCR in a panel of normal oral keratinocytes and oral cancer cells, relative to the internal endogenous control β -actin. In general, there is increased expression of most HOX genes, but particularly A4, A10, B9 and D10. **2B.** Expression of HOXB9 in a panel of NOK, OPM and HNSCC cells. **2C.** Expression of HOXB9 protein assayed by Western blotting for NOK cells compared to HNSCC (upper panel) and OPL (lower panel). * $p < 0.05$, ** $p < 0.01$, *** $p < 0.001$.

doi:10.1371/journal.pone.0122285.g002

was also seen in Western blot, with the HNSCCs and OPMs expressing more HOXB9 protein than NOK, (Fig 2C).

miR-196a and HOXB9 are more highly expressed in HNSCC tissues than in normal oral mucosa

The expression of miR-196a in tissues was assessed by qPCR of RNA extracted from laser-captured FFPE tissue. Whilst RNA from FFPE tissues is often degraded, the small size of micro-RNAs allows efficient recovery from fixed tissue [43]. Significantly higher expression of miR-196a was observed in 16 HNSCC tissues when compared to 16 unmatched normal mucosa (Fig 3A, $p < 0.05$), with some variation in expression seen in the normal samples. Analysis of HOXB9 expression by immunohistochemistry in a TMA containing 25 HNSCC samples compared with 10 normal oral mucosa samples revealed that this protein was more highly expressed in HNSCC compared to normal samples, as assessed by the Quickscore method (Fig 3B and 3C, $p < 0.001$). In normal tissues, expression of *HOXB9* was expressed at low levels, confined to the nuclei of the basal and spinous layers (Fig 3C Panel 1 and 2), whilst in HNSCC the nuclear intensity increased, with a greater proportion of cells in tumour nests expressing *HOXB9*

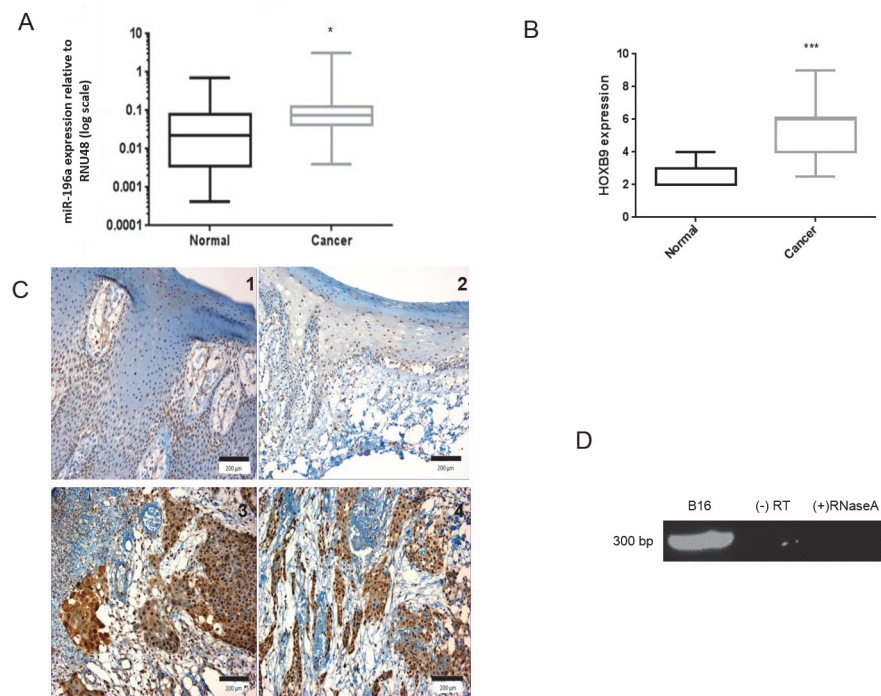


Fig 3. miR-196a and *HOXB9* are up-regulated in HNSCC tissue samples. 3A-C. Expression of miR-196a (3A) and *HOXB9* in tissues (3B, 3C) measured by qPCR of LCM tissues and immunohistochemistry, respectively. Representative photomicrographs show *HOXB9* expression in normal tissue (C panels 1 and 2) and HNSCC (C panels 3 and 4). The *HOXB9* expression in tissue was semi-quantitatively assessed using the Quickscore method. The pattern of expression correlates with *in-vitro* data and both are up-regulated in cancer tissue, albeit the fold change is less (3.4 fold for miR-196a). * $p < 0.05$, *** $p < 0.001$. Photomicrographs overall magnification x200, scale bar = 200 μm. 3D. miR-196a-1 and *HOXB9* are co-expressed on same novel primary transcript DNA agarose gel electrophoresis showing presence of 295 bp transcript after nested PCR. The transcript is present in B16 cell line and at the expected size. (-) RT: without reverse transcriptase control, (+) RNaseA: RNA treated with RNaseA at 37°C for 1 hour before cDNA production.

doi:10.1371/journal.pone.0122285.g003

(Fig 3C Panel 3 and 4). Furthermore, in the HNSCC tissues, there was cytoplasmic expression of HOXB9 in many cells.

HOXB9 and miR-196a-1 are co-transcribed on the same novel primary transcript

HOXB9 and miR-196a-1 are spatially closely related on Chr17. To show that HOXB9 and miR-196a-1 are co-transcribed on same primary transcript, primers were designed which spanned between HOXB9 exon 1 to miR-196a-1 precursor transcript (6.3 Kb). Nested primers were designed which amplified a 295bp region within this 6.3 Kb transcript (S1 Fig). A product of the expected molecular size was obtained (Fig 3D); no products were observed in the absence of reverse transcriptase (-RT) or following prolonged incubation with RNase A, suggesting this product is derived from a HOXB9-miR-196a-1 polycistronic primary transcript, rather than from genomic DNA contamination.

HOXB9 and miR-196a increase HNSCC cell migration and invasion

Given that both HOXB9 and miR-196a are highly expressed in HNSCC we assessed the phenotypic consequences of this in OPM and HNSCC cells, particularly assessing features that promote the ability of the cells to proliferate and to spread, enhancing the development of the tumour. Reducing expression of miR-196a or HOXB9 by anti-miR-196a (95% (B16) and 92% (D19)) and HOXB9 siRNA (62% (B16) and 48% (D19)), respectively (Figs 4A and 5A), reduced the ability of the OPM and HNSCC cells to migrate and invade into Matrigel (Figs 4C, 4D, 5C and 5D). The effects on proliferation and adhesion to fibronectin, a major component

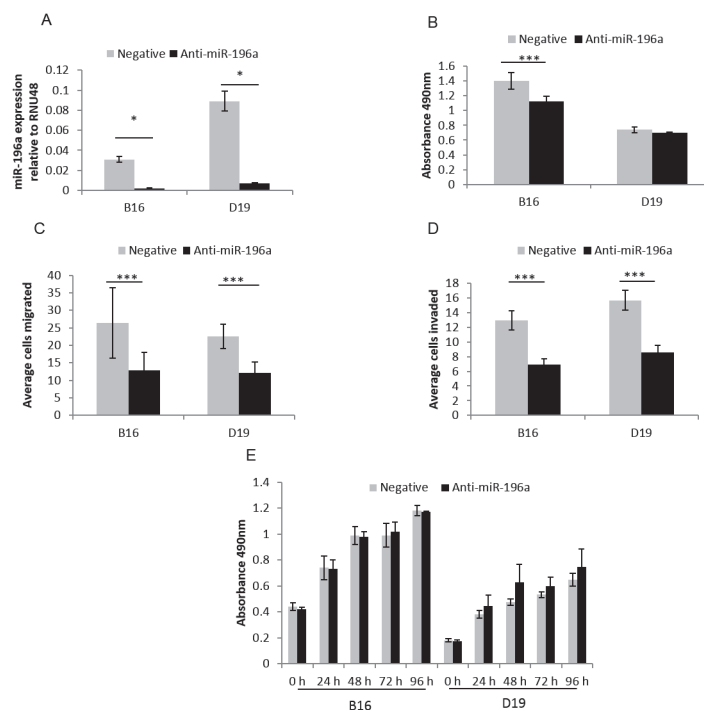


Fig 4. Functional effects of anti-miR-196a in HNSCC-derived cell lines. 4A. B16 and D19 cells were transfected with anti-miR-196a and negative control resulting in 95% and 92% reduction in miR-196a expression respectively compared to negative control. 4B-E. Anti-miR-196a decreases adhesion to fibronectin (B; in B16 only), migration (C), invasion (D) but has no effect on proliferation (E) in HNSCC cells. * p<0.05, *** p<0.001. All experiments were conducted in duplicate and completed three times.

doi:10.1371/journal.pone.0122285.g004

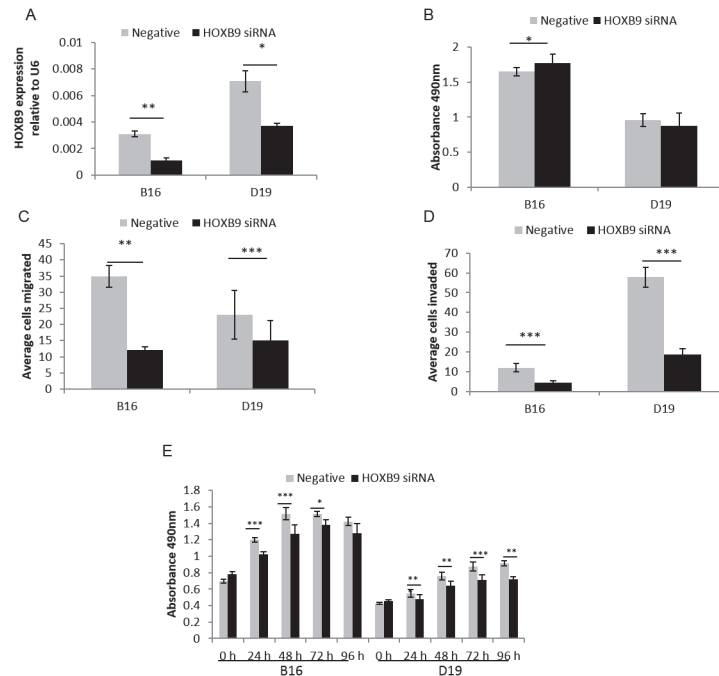


Fig 5. Functional effects of *HOXB9* siRNA in HNSCC-derived cell lines. 5A. B16 and D19 cells were transfected with *HOXB9* siRNA and negative control. There was 62% and 48% down-regulation seen in *HOXB9* expression compared to negative control in B16 and D19 respectively. 5B-E. *HOXB9* siRNA decreases migration (C), invasion (D) and proliferation (E) with no consistent change in adhesion to fibronectin (B) in HNSCC cells. * $p < 0.05$, ** $p < 0.01$, *** $p < 0.001$. All experiments were conducted in duplicate and completed three times.

doi:10.1371/journal.pone.0122285.g005

of the extracellular matrix, were more variable as reducing miR-196a expression reduced adhesion in HNSCC cells but not OPM cells, with no effect on proliferation in either cell type (Fig 4B and 4E). Supporting these observations, increased migration was seen after transfection of OKF4 (immortalised NOK) with pre-miR-196a, whilst there was no effect on proliferation or adhesion (data not shown). Reducing *HOXB9* expression by siRNA additionally reduced proliferation of OPM and HNSCC cells (Fig 5E). Adhesion to fibronectin was significantly increased in B16 only, but only to a small degree (Fig 5B).

Expression microarray analysis identifies known and putative miR-196a targets

Expression array data from both anti-miR (B16 and D19) and pre-miR (OKF4) transfected cells were used to identify consistent changes in gene expression related to alterations in miR-196a expression. This approach identified 353 altered genes ($p < 0.01$ by t-test) with the top 50 up- and down-regulated shown in Fig 6A. Gene Ontology (GO) enrichment analysis using DAVID (<http://david.abcc.ncifcrf.gov>) demonstrated a number of over-represented GO biological processes, including amine/amino acid transport, DNA repair and regulation of transcription (S5 Table). From this list, the top 20 up-regulated genes underwent further *in-silico* analysis for predicted miR-196a binding to the 3'UTR of each gene, to further focus the list to potential direct targets of miR-196a (Fig 6B). Other than *HOXC8* (S3D Fig), which has already been demonstrated to be a target of miR196a [18], the gene with the highest predicted interaction with miR-196a was MAM Domain Containing 2 (*MAMDC2*), which showed a good match based on sequence complementarity, energy of binding and evolutionary conservation

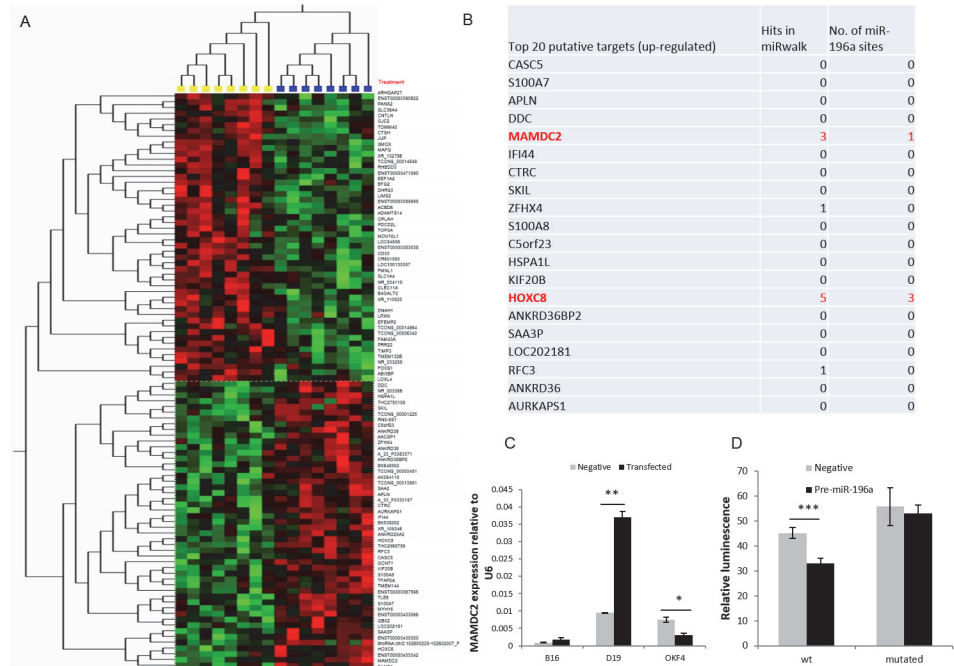


Fig 6. Prediction of putative targets of miR-196a in HNSCC-derived cell lines. **6A.** Microarray Heat Map depicting top 50 miR-196a up-regulated and down-regulated genes. Yellow samples were compared against blue samples (high and low miR-196a expression respectively) using Qlucore Omics Explorer with T-test, $p < 0.01$. Yellow box consists of B16 negative control, D19 negative control and OKF4 pre-miR-196a transfected cells whereas blue box consists of B16 anti-miR-196a, D19 anti-miR-196a and OKF4 negative control transfected cells. **6B.** Table depicting top 20 up-regulated putative targets based on expression analysis and miRwalk analysis of potential miRNA targets. It also shows number of miR-196a binding sites present in 3'UTR of the gene (www.microRNA.org) **6C:** The changes in *MAMDC2* expression on transfection of anti-miR-196a were validated by qPCR in samples used in microarray. **6D:** pMIR-REPORT luciferase vector was cloned with wild-type *MAMDC2* 3'UTR (wt) and the predicted miR-196a site in the 3'UTR was mutated by site-directed mutagenesis (mutated). These were co-transfected with negative control or pre-miR-196a, pRL-TK renilla luciferase control vector into B16 (HNSCC cells). The relative luminescence value (firefly/renilla value) of wt/pre-miR-196a was significantly lower than wt/negative control, with no significant difference in the mutated 3'UTR. * $p < 0.05$, ** $p < 0.01$, *** $p < 0.001$.

doi:10.1371/journal.pone.0122285.g006

of the site of 3'UTR to miR-196a (www.microrna.org). qPCR analysis of a number of reported miR196a targets in other cancers, *KRT5*, *ANXA1*, *S100A9* and *HOXC8*, was conducted ([S2 Fig](#)) [20,27]. These showed no consistent change on knockdown of miR196a in HNSCC and OPM cells, although *HOXC8* was differentially expressed in anti-miR196a transfected D19 cells.

MAMDC2 is a novel direct target of miR-196a

The change in *MAMDC2* expression seen on manipulation of miR-196a expression was validated by qPCR in the cells used in the microarray ([Fig 6C](#)). This confirmed the microarray data, showing *MAMDC2* expression increased after anti-miR-196a transfection in OPM ($p < 0.01$) and HNSCC ($p = 0.08$) cells and was reduced after pre-miR-196a transfection into immortalised NOK ($p < 0.05$). miR-196a over-expression significantly suppressed luciferase activity from a wild-type *MAMDC2* 3'UTR reporter construct in B16 cells ([Fig 6D](#)). This suppression was not observed following mutation of the predicted miR-196a binding site ([Fig 6D](#)), indicating a direct effect of miR-196a on *MAMDC2* expression at a transcript level.

Discussion

There is now considerable evidence that miR-196a and HOXB9 exert a pro-tumorigenic influence in many cancers [13,15,22,27]. Our data convincingly demonstrate high expression of both miR-196a and *HOXB9* in HNSCC and in at least a subset of OPMs. This is in keeping with recent studies in HNSCC and also a number of other cancers, including breast and non-small cell lung carcinoma (NSCLC) [5,7,22,28,30,44]. Furthermore, a key role for miR-196a polymorphisms has emerged in relation to cancer risk, conferring increased susceptibility to a number of cancers, particularly in Asian populations [45]. Despite a well-recognised role in invasive disease, the function of miR-196a overexpression in the pre-invasive stage of HNSCC development has not been investigated before. We found high miR-196a expression in some OPM samples, whilst in others the level of expression is similar to NOK. Further investigations will be required to define the role of this overexpression and whether OPMs with high miR-196a expression progress to HNSCC.

Recent investigations in oral carcinomas have also demonstrated a pro-tumorigenic phenotype in cells expressing high levels of miR-196a, and this has been linked to poor patient outcome, with similar effects seen in NSCLC and gastric cancer [16,25]. Liu et al showed overexpression of miR-196a in HNSCC cells had little effect on tumour cell proliferation, but did result in an increase in cell migration [22], which is in keeping with our findings and also those seen on manipulation of miR-196a expression in a number of other cancer cell types [46]. Conversely, overexpression of miR-196a in NOKs resulted in a marked reduction in proliferation [30], but it is difficult to directly compare these effects with those seen in HNSCC cells given the markedly different genomic and transcriptomic background. Our investigations of transfection of pre-miR-196a into the immortalised NOK cell line OKF4 showed no change in proliferation and a small increase in migration (data not shown).

HOXB9 expression is elevated in a range of cancers including breast, NSCLC and hepatocellular carcinoma [5,7,47], but decreased expression has been related to poor prognosis in others [48]. The increased expression of *HOXB9* in HNSCC which we have demonstrated *in vitro* and in tissues has also been shown in a small number of other microarray analyses and in comparable qPCR assessment of *HOX* gene expression in HNSCC [17,49,50]. The identification of the differential expression of *HOXB9* in HNSCC in the array analysis of Ginos et al [49] is notable as *HOXB9* was not identified in the original Hunter et al dataset [3], but was shown in this study by qPCR (Fig 2). This illustrates the limitations of many expression array analyses given the variability of samples analysed and uncertainties surrounding the probesets which have been used to detect the targets. For the first time we have demonstrated increased *HOXB9* expression in OPM cultures, which was not seen in the investigation of Hassan et al [17]. However, 3 of the 4 cultures we used were derived from severely dysplastic lesions which progressed to HNSCC in less than 6 months (D19, D20 and D35). This indicates that a more detailed analysis of the expression and role of *HOXB9* in OPM is warranted to determine if expression of *HOXB9* increases with OPM severity.

We have shown that *HOXB9* enhances migration, invasion and proliferation of both HNSCC and OPM cells in keeping with the effects of high *HOXB9* expression in other cancers, but which has not been demonstrated previously in HNSCC or in pre-invasive disease. Our findings are in keeping with the observed increase in migration and invasion in breast cancer, where elevated *HOXB9* expression enhances the DNA damage response, not only conferring resistance to ionizing radiation, but also associated with induction of epithelial to mesenchymal transition (EMT) [51]. Investigations in other cancers have demonstrated similar roles in addition to enhancement of tumour proliferation and angiogenesis [13,52]. These are important

issues to address in relation to both miR196a and HOXB9 and we are currently undertaking further investigation of the mechanisms of altered migration and invasion.

The apparent similarity in the patterns of expression of *HOXB9* and miR-196a has been demonstrated in Hodgkin lymphoma and AML cells, suggesting co-regulation, but in neither case were further investigations conducted [53,54]. The presence of numerous polycistronic transcripts from the *HOX* loci has been inferred from analysis of high resolution transcriptional profiling, including a putative transcript which includes *HOXB7*, *HOXB8*, *HOXB9* and miR-196a-1 [55]. This transcript is annotated in Ensembl (Transcript: RP11-357H14.19-001), without direct experimental evidence of its existence. We have demonstrated the existence of a transcript that at least spans the 6.3kb region between the open reading frames of *HOXB9* and miR-196a-1. However, what is not clear is what proportion of *HOXB9* and miR-196a expression is accounted for by this transcript. Given that the expression of *HOXB9* and miR-196a is not completely coordinated, particularly in OPM cells (Figs 2B and 1C), it is likely that this transcript only contributes a proportion of the pool of processed mRNA for *HOXB9* and miR-196a, indicating that, whilst there may be co-expression, expression of *HOXB9* and miR-196a is under the control of other factors, which remain to be elucidated, which are responsible for different transcripts. An understanding of the primary transcripts used in the expression of both *HOXB9* and miR-196a will be important in directing possible approaches to inhibition.

There are significant difficulties in the identification of endogenous miRNA targets and this has led to the use of a wide range of techniques, ranging from *in-silico* methods to direct assessment of binding between the miRNA seed sequence and binding site in the 3'UTR of cognate mRNAs. We decided to pursue novel targets of miR-196a by expression microarray following miR-196a over-expression and knockdown, despite the acknowledged limitations of this approach, including possible effects on protein and not mRNA. The microarray expression data and subsequent *in-silico* analysis identified a number of potential targets of miR-196a, including some which have been identified in other cell types, such as *HOXC8* (S3 Fig) [18]. However, the overall GO enrichment analysis only identified a small number of enriched biological processes that were affected by manipulation of miR-196a expression. The most enriched categories included DNA repair, the DNA damage response and various transporter pathways (S1 Table). These do not appear to map directly to the observed phenotype, which may be partly due to the relatively small number of differentially expressed genes identified and also demonstrate the interaction of miR-196a in controlling a wide range of different processes in the cell. Interestingly, we observed no consistent changes in the expression of miR-196a targets which have been identified in other cancer types. This may indicate a level of tumour specificity in the actions of miR-196a.

Overall, the highest ranked novel gene target in our analysis was MAMDC2. The level of MAMDC2 expression varies between the NOK, OPM and HNSCC cells, indicative of control of expression by other, as yet unknown mechanisms. However, given the effect on transfection of pre-miR196 or anti-miR196 presented in Fig 6C and 6D, there is good evidence that MAMDC2 is under the direct control of miR196a. MAMDC2 is a transmembrane cell adhesion protein of the immunoglobulin superfamily. MAM (meprin/A5-protein/PTPmu) domains are present in numerous proteins with varied functions, with many associated with promotion of cell-cell adhesion [56,57]. Correspondingly, mutations in the MAM domain of the receptor protein tyrosine phosphatase T have been shown to promote cancer cell migration and metastasis in colorectal cancer [58,59]. Whilst this would be in keeping with the phenotype observed upon transfection with anti-miR-196a, this requires further investigation to establish if this observation can be attributed to the biological functions of MAMDC2. Given that a number of small molecules which interfere with cell adhesion are currently being tested as anti-cancer agents, this may also represent a novel therapeutic target.

Given that elevated *HOXB9* expression and high serum levels of miR-196a have been associated with poor prognosis and recurrence in other tumour types [5,7,16], it is conceivable, that together, they may be of prognostic use in HNSCC. Potential therapeutic applications may be more challenging as, whilst inhibitors of the *HOX-PBX* interaction are available and effective [8], some of the 5' *HOX* genes (e.g. *HOXD10* and *HOXB9*) are less PBX dependent which may limit their use [60], thus new strategies for disruption of this interaction may prove more effective. Furthermore, if the molecular mechanisms responsible for the transcription of the novel primary transcript identified here can be elucidated, it may be possible to inhibit its expression and subsequent effects.

Conclusions

In this manuscript we have demonstrated that both *HOXB9* and miR196a are highly expressed in HNSCC both *in vivo* and *in vitro*. Both exert a pro-tumour phenotype and we have demonstrated a putative primary transcript which bears both coding sequences. This suggests that inhibition of expression of genes across this locus may prove a useful therapeutic strategy as this will inhibit a number of pro-tumorigenic factors. Furthermore we have identified *MAMDC2* as a novel target of miR196a in HNSCC, suggesting further interrogation of the biological significance of the miR-196a/*MAMDC2* axis may enhance understanding of HNSCC pathogenesis.

Supporting Information

S1 Fig. Schematic diagram of the putative primary transcript and the length of the PCR product for both the primers utilised in the nested PCR analysis.

(TIF)

S2 Fig. Expression of all *HOX* genes analysed by qPCR, showing data in the full panel of cell cultures tested, including normal (black), OPM (red) and HNSCC (blue), arranged by group (A-D) and in numerical order.

(TIF)

S3 Fig. Expression of putative miR196a targets suggested from investigation in other cancers, as assessed by qPCR in anti-miR196a transfected D19 and B16 cells, and pre-miR196a transfected OKF4 cells in panel D. A: Keratin V; B: Anxin A1; C S100A9; D: HOXC8. Only HOXC8 shows significant changes in expression and this only in D19 ($p < 0.01$). The data does not support regulation of KRT5, ANXA1 or S100A9 by miR196a in HNSCC.

(TIF)

S1 Table. Clinical details of the HNSCC and OPM cell lines used in this study. All cell lines are HPV negative.

(DOCX)

S2 Table. Clinical and pathological details of the 25 HNSCC samples in the TMA used for *HOXB9* IHC. FOM = Floor of mouth, RM = retromolar, BM = buccal mucosa.

(DOCX)

S3 Table. Clinical pathological details of HNSCC samples used for Laser capture microdissection FOM = Floor of mouth, RM = retromolar, BM = buccal mucosa.

(DOCX)

S4 Table. A full list of qPCR primers used in this study.

(DOCX)

S5 Table. Gene ontology enrichment analysis demonstrating significantly enriched GO biological processes on manipulation of miR-196a expression. The total number of significantly differentially expressed genes entered into this analysis was 353. Analysis generated by analysis of the gene list in DAVID (<http://david.abcc.ncifcrf.gov>). (DOCX)

Author Contributions

Conceived and designed the experiments: LD FH RM CM DWL KDH. Performed the experiments: LD FH. Analyzed the data: LD FH RM CM DWL KDH. Contributed reagents/materials/analysis tools: CR CM DWL KDH. Wrote the paper: LD FH RM CM DWL KDH.

References

1. Markovic A, Chung CH (2012) Current role of EGF receptor monoclonal antibodies and tyrosine kinase inhibitors in the management of head and neck squamous cell carcinoma. *Expert Rev Anticancer Ther* 12: 1149–1159. doi: [10.1586/era.12.91](https://doi.org/10.1586/era.12.91) PMID: [23098115](https://pubmed.ncbi.nlm.nih.gov/23098115/)
2. Leemans CR, Braakhuis BJ, Brakenhoff RH (2011) The molecular biology of head and neck cancer. *Nat Rev Cancer* 11: 9–22. doi: [10.1038/nrc2982](https://doi.org/10.1038/nrc2982) PMID: [21160525](https://pubmed.ncbi.nlm.nih.gov/21160525/)
3. Hunter KD, Thurlow JK, Fleming J, Drake PJ, Vass JK, et al. (2006) Divergent routes to oral cancer. *Cancer Res* 66: 7405–7413. PMID: [16885335](https://pubmed.ncbi.nlm.nih.gov/16885335/)
4. Grier DG, Thompson A, Kwasniewska A, McGonigle GJ, Halliday HL, et al. (2005) The pathophysiology of HOX genes and their role in cancer. *J Pathol* 205: 154–171. PMID: [15643670](https://pubmed.ncbi.nlm.nih.gov/15643670/)
5. Calvo R, West J, Franklin W, Erickson P, Bemis L, et al. (2000) Altered HOX and WNT7A expression in human lung cancer. *Proc Natl Acad Sci U S A* 97: 12776–12781. PMID: [11070089](https://pubmed.ncbi.nlm.nih.gov/11070089/)
6. Barber BA, Rastegar M (2010) Epigenetic control of Hox genes during neurogenesis, development, and disease. *Ann Anat* 192: 261–274. doi: [10.1016/j.aanat.2010.07.009](https://doi.org/10.1016/j.aanat.2010.07.009) PMID: [20739155](https://pubmed.ncbi.nlm.nih.gov/20739155/)
7. Hayashida T, Takahashi F, Chiba N, Brachtel E, Takahashi M, et al. (2010) HOXB9, a gene overexpressed in breast cancer, promotes tumorigenicity and lung metastasis. *Proc Natl Acad Sci U S A* 107: 1100–1105. doi: [10.1073/pnas.0912710107](https://doi.org/10.1073/pnas.0912710107) PMID: [20080567](https://pubmed.ncbi.nlm.nih.gov/20080567/)
8. Morgan R, Plowright L, Harrington KJ, Michael A, Pandha HS (2010) Targeting HOX and PBX transcription factors in ovarian cancer. *BMC Cancer* 10: 89. doi: [10.1186/1471-2407-10-89](https://doi.org/10.1186/1471-2407-10-89) PMID: [20219106](https://pubmed.ncbi.nlm.nih.gov/20219106/)
9. Taketani T, Taki T, Shibuya N, Kikuchi A, Hanada R, et al. (2002) Novel NUP98-HOXC11 fusion gene resulted from a chromosomal break within exon 1 of HOXC11 in acute myeloid leukemia with t(11;12)(p15;q13). *Cancer Res* 62: 4571–4574. PMID: [12183408](https://pubmed.ncbi.nlm.nih.gov/12183408/)
10. Raza-Egilmez SZ, Jani-Sait SN, Grossi M, Higgins MJ, Shows TB, et al. (1998) NUP98-HOXD13 gene fusion in therapy-related acute myelogenous leukemia. *Cancer Res* 58: 4269–4273. PMID: [9766650](https://pubmed.ncbi.nlm.nih.gov/9766650/)
11. Raman V, Martensen SA, Reisman D, Evron E, Odenwald WF, et al. (2000) Compromised HOXA5 function can limit p53 expression in human breast tumours. *Nature* 405: 974–978. PMID: [10879542](https://pubmed.ncbi.nlm.nih.gov/10879542/)
12. Rodriguez BA, Cheng AS, Yan PS, Potter D, Agosto-Perez FJ, et al. (2008) Epigenetic repression of the estrogen-regulated Homeobox B13 gene in breast cancer. *Carcinogenesis* 29: 1459–1465. doi: [10.1093/carcin/bgn115](https://doi.org/10.1093/carcin/bgn115) PMID: [18499701](https://pubmed.ncbi.nlm.nih.gov/18499701/)
13. Seki H, Hayashida T, Jinno H, Hirose S, Sakata M, et al. (2012) HOXB9 expression promoting tumor cell proliferation and angiogenesis is associated with clinical outcomes in breast cancer patients. *Ann Surg Oncol* 19: 1831–1840. doi: [10.1245/s10434-012-2295-5](https://doi.org/10.1245/s10434-012-2295-5) PMID: [22396001](https://pubmed.ncbi.nlm.nih.gov/22396001/)
14. Plowright L, Harrington KJ, Pandha HS, Morgan R (2009) HOX transcription factors are potential therapeutic targets in non-small-cell lung cancer (targeting HOX genes in lung cancer). *Br J Cancer* 100: 470–475. doi: [10.1038/sj.bjc.6604857](https://doi.org/10.1038/sj.bjc.6604857) PMID: [19156136](https://pubmed.ncbi.nlm.nih.gov/19156136/)
15. Nguyen DX, Chiang AC, Zhang XH, Kim JY, Kris MG, et al. (2009) WNT/TCF signaling through LEF1 and HOXB9 mediates lung adenocarcinoma metastasis. *Cell* 138: 51–62. doi: [10.1016/j.cell.2009.04.030](https://doi.org/10.1016/j.cell.2009.04.030) PMID: [19576624](https://pubmed.ncbi.nlm.nih.gov/19576624/)
16. Tsai KW, Liao YL, Wu CW, Hu LY, Li SC, et al. (2012) Aberrant expression of miR-196a in gastric cancers and correlation with recurrence. *Genes Chromosomes Cancer* 51: 394–401. PMID: [22420029](https://pubmed.ncbi.nlm.nih.gov/22420029/)
17. Hassan N, Hamada J, Murai T, Seino A, Takahashi Y, et al. (2006) Aberrant expression of HOX genes in oral dysplasia and squamous cell carcinoma tissues. *Oncol Res* 16: 217–224. PMID: [17294802](https://pubmed.ncbi.nlm.nih.gov/17294802/)

18. Li Y, Zhang M, Chen H, Dong Z, Ganapathy V, et al. (2010) Ratio of miR-196s to HOXC8 messenger RNA correlates with breast cancer cell migration and metastasis. *Cancer Res* 70: 7894–7904. doi: [10.1158/0008-5472.CAN-10-1675](https://doi.org/10.1158/0008-5472.CAN-10-1675) PMID: [20736365](https://pubmed.ncbi.nlm.nih.gov/20736365/)
19. Asli NS, Kessel M (2010) Spatiotemporally restricted regulation of generic motor neuron programs by miR-196-mediated repression of Hoxb8. *Dev Biol* 344: 857–868. doi: [10.1016/j.ydbio.2010.06.003](https://doi.org/10.1016/j.ydbio.2010.06.003) PMID: [20553899](https://pubmed.ncbi.nlm.nih.gov/20553899/)
20. Maru DM, Singh RR, Hannah C, Albarracin CT, Li YX, et al. (2009) MicroRNA-196a is a potential marker of progression during Barrett's metaplasia-dysplasia-invasive adenocarcinoma sequence in esophagus. *Am J Pathol* 174: 1940–1948. doi: [10.2353/ajpath.2009.080718](https://doi.org/10.2353/ajpath.2009.080718) PMID: [19342367](https://pubmed.ncbi.nlm.nih.gov/19342367/)
21. McGlenn E, Yekta S, Mansfield JH, Soutschek J, Bartel DP, et al. (2009) In ovo application of antagonistic miRNAs indicates a role for miR-196 in patterning the chick axial skeleton through Hox gene regulation. *Proc Natl Acad Sci U S A* 106: 18610–18615. doi: [10.1073/pnas.0910374106](https://doi.org/10.1073/pnas.0910374106) PMID: [19846767](https://pubmed.ncbi.nlm.nih.gov/19846767/)
22. Liu CJ, Tsai MM, Tu HF, Lui MT, Cheng HW, et al. (2012) miR-196a Overexpression and miR-196a2 Gene Polymorphism Are Prognostic Predictors of Oral Carcinomas. *Ann Surg Oncol*.
23. Yekta S, Shih IH, Bartel DP (2004) MicroRNA-directed cleavage of HOXB8 mRNA. *Science* 304: 594–596. PMID: [15105502](https://pubmed.ncbi.nlm.nih.gov/15105502/)
24. Braig S, Mueller DW, Rothhammer T, Bosserhoff AK (2010) MicroRNA miR-196a is a central regulator of HOX-B7 and BMP4 expression in malignant melanoma. *Cell Mol Life Sci* 67: 3535–3548. doi: [10.1007/s00018-010-0394-7](https://doi.org/10.1007/s00018-010-0394-7) PMID: [20480203](https://pubmed.ncbi.nlm.nih.gov/20480203/)
25. Liu XH, Lu KH, Wang KM, Sun M, Zhang EB, et al. (2012) MicroRNA-196a promotes non-small cell lung cancer cell proliferation and invasion through targeting HOXA5. *BMC Cancer* 12: 348. doi: [10.1186/1471-2407-12-348](https://doi.org/10.1186/1471-2407-12-348) PMID: [22876840](https://pubmed.ncbi.nlm.nih.gov/22876840/)
26. Sun M, Liu XH, Li JH, Yang JS, Zhang EB, et al. (2012) MiR-196a is upregulated in gastric cancer and promotes cell proliferation by downregulating p27(kip1). *Mol Cancer Ther* 11: 842–852. doi: [10.1158/1535-7163.MCT-11-1015](https://doi.org/10.1158/1535-7163.MCT-11-1015) PMID: [22343731](https://pubmed.ncbi.nlm.nih.gov/22343731/)
27. Luthra R, Singh RR, Luthra MG, Li YX, Hannah C, et al. (2008) MicroRNA-196a targets annexin A1 downregulation in cancers. *Oncogene* 27: 6667–6678. doi: [10.1038/onc.2008.256](https://doi.org/10.1038/onc.2008.256) PMID: [18663355](https://pubmed.ncbi.nlm.nih.gov/18663355/)
28. Hui AB, Shi W, Boutros PC, Miller N, Pintilie M, et al. (2009) Robust global micro-RNA profiling with formalin-fixed paraffin-embedded breast cancer tissues. *Lab Invest* 89: 597–606. doi: [10.1038/labinvest.2009.12](https://doi.org/10.1038/labinvest.2009.12) PMID: [19290006](https://pubmed.ncbi.nlm.nih.gov/19290006/)
29. Mueller DW, Bosserhoff AK (2011) MicroRNA miR-196a controls melanoma-associated genes by regulating HOX-C8 expression. *Int J Cancer* 129: 1064–1074. doi: [10.1002/ijc.25768](https://doi.org/10.1002/ijc.25768) PMID: [21077158](https://pubmed.ncbi.nlm.nih.gov/21077158/)
30. Severino P, Bruggemann H, Andreghetto FM, Camps C, Klingbeil Mde F, et al. (2013) MicroRNA expression profile in head and neck cancer: HOX-cluster embedded microRNA-196a and microRNA-10b dysregulation implicated in cell proliferation. *BMC Cancer* 13: 533. doi: [10.1186/1471-2407-13-533](https://doi.org/10.1186/1471-2407-13-533) PMID: [24209638](https://pubmed.ncbi.nlm.nih.gov/24209638/)
31. Burns J, Baird M, Clark L, Burns P, Edington K, et al. (1993) Gene mutations and increased levels of p53 protein in human squamous cell carcinomas and their cell lines. *British Journal of Cancer* 67: 1274–1284. PMID: [8390283](https://pubmed.ncbi.nlm.nih.gov/8390283/)
32. Burns JE, McFarlane R, Clark LJ, Mitchell R, Robertson G, et al. (1994) Maintenance of identical p53 mutations throughout progression of squamous cell carcinomas of the tongue. *Eur J Cancer B Oral Oncol* 30B: 335–337. PMID: [7703803](https://pubmed.ncbi.nlm.nih.gov/7703803/)
33. Prime SS, Nixon SV, Crane IJ, Stone A, Matthews JB, et al. (1990) The behaviour of human oral squamous cell carcinoma in cell culture. *J Pathol* 160: 259–269. PMID: [1692339](https://pubmed.ncbi.nlm.nih.gov/1692339/)
34. McGregor F, Muntoni A, Fleming J, Brown J, Felix DH, et al. (2002) Molecular changes associated with oral dysplasia progression and acquisition of immortality: potential for its reversal by 5-azacytidine. *Cancer Res* 62: 4757–4766. PMID: [12183435](https://pubmed.ncbi.nlm.nih.gov/12183435/)
35. McGregor F, Wagner E, Felix D, Soutar D, Parkinson K, et al. (1997) Inappropriate retinoic and receptor β expression in oral dysplasias: correlation with acquisition of the immortal phenotype. *Cancer research* 57: 3886–3889. PMID: [9307265](https://pubmed.ncbi.nlm.nih.gov/9307265/)
36. Colley HE, Hearnden V, Jones AV, Weinreb PH, Violette SM, et al. (2011) Development of tissue-engineered models of oral dysplasia and early invasive oral squamous cell carcinoma. *Br J Cancer* 105: 1582–1592. doi: [10.1038/bjc.2011.403](https://doi.org/10.1038/bjc.2011.403) PMID: [21989184](https://pubmed.ncbi.nlm.nih.gov/21989184/)
37. Dickson MA, Hahn WC, Ino Y, Ronfard V, Wu JY, et al. (2000) Human keratinocytes that express hTERT and also bypass a p16(INK4a)-enforced mechanism that limits life span become immortal yet retain normal growth and differentiation characteristics. *Mol Cell Biol* 20: 1436–1447. PMID: [10648628](https://pubmed.ncbi.nlm.nih.gov/10648628/)
38. Smith PK, Krohn RI, Hermanson GT, Mallia AK, Gartner FH, et al. (1985) Measurement of protein using bicinchoninic acid. *Anal Biochem* 150: 76–85. PMID: [3843705](https://pubmed.ncbi.nlm.nih.gov/3843705/)

39. Neves JI, Begnami MD, Arias V, Santos GC (2005) Antigen retrieval methods and estrogen receptor immunoexpression using 1D5 antibody: a comparative study. *Int J Surg Pathol* 13: 353–357. PMID: [16273191](#)
40. Detre S, Saclani Jotti G, Dowsett M (1995) A "quickscore" method for immunohistochemical semiquantitation: validation for oestrogen receptor in breast carcinomas. *J Clin Pathol* 48: 876–878. PMID: [7490328](#)
41. Mao L, Ding J, Zha Y, Yang L, McCarthy BA, et al. (2011) HOXC9 links cell-cycle exit and neuronal differentiation and is a prognostic marker in neuroblastoma. *Cancer Res* 71: 4314–4324. doi: [10.1158/0008-5472.CAN-11-0051](#) PMID: [21507931](#)
42. Drabkin HA, Parsy C, Ferguson K, Guilhot F, Lacotte L, et al. (2002) Quantitative HOX expression in chromosomally defined subsets of acute myelogenous leukemia. *Leukemia* 16: 186–195. PMID: [11840284](#)
43. Nonn L, Vaishnav A, Gallagher L, Gann PH (2010) mRNA and micro-RNA expression analysis in laser-capture microdissected prostate biopsies: valuable tool for risk assessment and prevention trials. *Exp Mol Pathol* 88: 45–51. doi: [10.1016/j.yexmp.2009.10.005](#) PMID: [19874819](#)
44. Chen Z, Jin Y, Yu D, Wang A, Mahjabeen I, et al. (2012) Down-regulation of the microRNA-99 family members in head and neck squamous cell carcinoma. *Oral Oncol* 48: 686–691. doi: [10.1016/j.oraloncology.2012.02.020](#) PMID: [22425712](#)
45. Zhang H, Su YL, Yu H, Qian BY (2012) Meta-Analysis of the Association between Mir-196a-2 Polymorphism and Cancer Susceptibility. *Cancer Biol Med* 9: 63–72. doi: [10.3969/j.issn.2095-3941.2012.01.012](#) PMID: [23691458](#)
46. Tsai MM, Wang CS, Tsai CY, Chen CY, Chi HC, et al. (2014) MicroRNA-196a/-196b promote cell metastasis via negative regulation of radixin in human gastric cancer. *Cancer Lett* 351: 222–231. doi: [10.1016/j.canlet.2014.06.004](#) PMID: [24933454](#)
47. Kanai M, Hamada J, Takada M, Asano T, Murakawa K, et al. (2010) Aberrant expressions of HOX genes in colorectal and hepatocellular carcinomas. *Oncol Rep* 23: 843–851. PMID: [20127028](#)
48. Sha S, Gu Y, Xu B, Hu H, Yang Y, et al. (2013) Decreased expression of HOXB9 is related to poor overall survival in patients with gastric carcinoma. *Dig Liver Dis*.
49. Ginos MA, Page GP, Michalowicz BS, Patel KJ, Volker SE, et al. (2004) Identification of a gene expression signature associated with recurrent disease in squamous cell carcinoma of the head and neck. *Cancer Res* 64: 55–63. PMID: [14729608](#)
50. Walter V, Yin X, Wilkerson MD, Cabanski CR, Zhao N, et al. (2013) Molecular subtypes in head and neck cancer exhibit distinct patterns of chromosomal gain and loss of canonical cancer genes. *PLoS One* 8: e56823. doi: [10.1371/journal.pone.0056823](#) PMID: [23451093](#)
51. Chiba N, Comaills V, Shiotani B, Takahashi F, Shimada T, et al. (2012) Homeobox B9 induces epithelial-to-mesenchymal transition-associated radioresistance by accelerating DNA damage responses. *Proc Natl Acad Sci U S A* 109: 2760–2765. doi: [10.1073/pnas.1018867108](#) PMID: [21930940](#)
52. Sha L, Dong L, Lv L, Bai L, Ji X (2014) HOXB9 promotes epithelial-to-mesenchymal transition via transforming growth factor-beta1 pathway in hepatocellular carcinoma cells. *Clin Exp Med*.
53. Nagel S, Burek C, Venturini L, Scherr M, Quentmeier H, et al. (2007) Comprehensive analysis of homeobox genes in Hodgkin lymphoma cell lines identifies dysregulated expression of HOXB9 mediated via ERK5 signaling and BMI1. *Blood* 109: 3015–3023. PMID: [17148583](#)
54. Danen-van Oorschot AA, Kuipers JE, Arentsen-Peters S, Schotte D, de Haas V, et al. (2012) Differentially expressed miRNAs in cytogenetic and molecular subtypes of pediatric acute myeloid leukemia. *Pediatr Blood Cancer* 58: 715–721. doi: [10.1002/pbc.23279](#) PMID: [21818844](#)
55. Mainguy G, Koster J, Woltering J, Jansen H, Durston A (2007) Extensive polycistronism and antisense transcription in the mammalian Hox clusters. *PLoS One* 2: e356. PMID: [17406680](#)
56. Cismasiu VB, Denes SA, Reilander H, Michel H, Szedlacsek SE (2004) The MAM (meprin/A5-protein/PTPmu) domain is a homophilic binding site promoting the lateral dimerization of receptor-like protein-tyrosine phosphatase mu. *J Biol Chem* 279: 26922–26931. PMID: [15084579](#)
57. Diaz-Lopez A, Iniesta P, Moran A, Ortega P, Fernandez-Marcelo T, et al. (2010) Expression of Human MDGA1 Increases Cell Motility and Cell-Cell Adhesion and Reduces Adhesion to Extracellular Matrix Proteins in MDCK Cells. *Cancer Microenviron* 4: 23–32. doi: [10.1007/s12307-010-0055-2](#) PMID: [21505559](#)
58. Zhang P, Becka S, Craig SE, Lodowski DT, Brady-Kalnay SM, et al. (2009) Cancer-derived mutations in the fibronectin III repeats of PTPRT/PTPrho inhibit cell-cell aggregation. *Cell Commun Adhes* 16: 146–153. doi: [10.3109/15419061003653771](#) PMID: [20230342](#)

59. Yu J, Becka S, Zhang P, Zhang X, Brady-Kalnay SM, et al. (2008) Tumor-derived extracellular mutations of PTPRT /PTPrho are defective in cell adhesion. *Mol Cancer Res* 6: 1106–1113. doi: [10.1158/1541-7786.MCR-07-2123](https://doi.org/10.1158/1541-7786.MCR-07-2123) PMID: [18644975](https://pubmed.ncbi.nlm.nih.gov/18644975/)
60. Pan W (2002) A comparative review of statistical methods for discovering differentially expressed genes in replicated microarray experiments. *Bioinformatics* 18: 546–554. PMID: [12016052](https://pubmed.ncbi.nlm.nih.gov/12016052/)